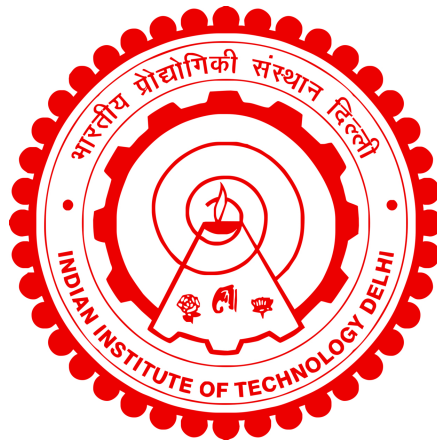


# MICROSCALE FLOWS OVER PATTERNED TOPOGRAPHIES

MAINENDRA KUMAR DEWANGAN



DEPARTMENT OF MECHANICAL ENGINEERING  
INDIAN INSTITUTE OF TECHNOLOGY DELHI  
OCTOBER 2020

© Indian Institute of technology Delhi (IITD), New Delhi, 2020

# MICROSCALE FLOWS OVER PATTERNED TOPOGRAPHIES

by

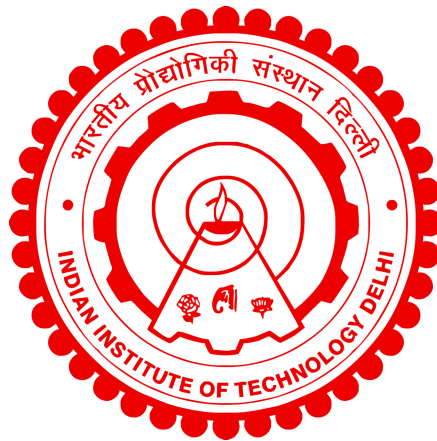
**MAINENDRA KUMAR DEWANGAN**

Department of Mechanical Engineering

Submitted

in partial fulfillment of the requirements of the degree of Doctor of Philosophy

to the



**INDIAN INSTITUTE OF TECHNOLOGY DELHI**  
**OCTOBER 2020**

Dedicated to my parents. This would have not been possible without your patience and  
endless support.

# Certificate

This is to certify that the thesis entitled “**Microscale flows over patterned topographies**” being submitted by **Mr. Mainendra Kumar Dewangan** to the Indian Institute of Technology, Delhi for the award of the degree of **Doctor of Philosophy** is a bonafide record of original research work carried out by him under my supervision in conformity with rules and regulations of the institute. The results contained in this thesis have not been submitted, in part or in full, to any other University or Institute for the award of any Degree or Diploma.

Dr. Subhra Datta  
Associate Professor  
Department of Mechanical Engineering,  
Indian Institute of Technology Delhi,  
New Delhi-110016, India

# Acknowledgements

First of all, I thank my thesis supervisor, Prof. Subhra Datta, who provided me an opportunity to conduct research work in the area of micro-/nanoscale liquid flows. I would like to express my sincere gratitude to him for his constant guidance, encouragement, regular discussion, and enthusiasm throughout the research work. I would like to appreciate his patience in correcting my technical and linguistic errors in the manuscript of the thesis. I would like to thank the chairman of SRC, Prof. P.M.V. Subbarao, and the other members Prof. Amit Gupta and Prof. Arghya Samanta, for their critical reviews and valuable suggestions.

I am very much thankful to Dr. Saurabh Chandrakar, Dr. Girish Verma, Dr. Manjinder, and Dr. Rattandeep for their help during the initial stage of my doctoral work and continued support throughout the entire phase of the project work. I wish to thank Mr. Kaushlendra for his informative discussions on the micro and nano fluidics.

I am especially grateful to my lab mates and hostel friends Mr. Abhinava, Mr. Devershi, Mr. Ashutosh, Mr. Vishal, and Mr. Abhishek for care, encouragement and support provided by them. I am indebted to many student colleagues of mine for providing me with a fun filled environment in the hostel. I am very much thankful to IIT Delhi computer center for Computing Resources for providing us with COMSOL Multiphysics, Matlab and Mathematica licenses.

Finally, I would like to express my heartfelt gratitude to my parents for their support, encouragement and boundless love during all these years of education and to all my teachers starting from primary school to those at IIT Delhi, who actually have motivated and brought me to the present position.

**Mainendra Kumar Dewangan**

# Abstract

Topographical textures or surface corrugations are often employed in the discipline of microfluidics to achieve objectives such as mixing, modulation of wetting and frictional properties, and separations. Outside microfluidics, such textures form the basis of drag-reducing riblets engineered to turbulent flows and are natural features of fractured rocks carrying oil or water in geological formations.

Motivated by such applications, macroscopic characterization of creeping Newtonian flows establishing wetted contact with topographies is undertaken theoretically, using the effective slip length tensor as a metric for unconfined flows and the hydraulic permeability tensor as a metric for confined flows. Flows longitudinal as well as transverse to one-dimensional grooved/striped patterns are analyzed using spectral and asymptotic methods. Continuum scale fully resolved finite-element simulations are employed to assess the usefulness of asymptotic predictions. The main asymptotic approach used in this thesis treats the ratio of the characteristic size of the topographical pattern to the pattern pitch as a small parameter, the dimensionless amplitude.

First, for sinusoidally corrugated no-slip surfaces in shear flow, analytical models usable over a significantly wider amplitude range than those available from the literature are developed, taking advantages of symbolic computations, numerical-graphical convergence studies with Domb-Sykes plots and series-improvement techniques like Euler and Shanks transformation and Padé approximants.

Next, flows over corrugated surfaces with intrinsic slippage are studied. To understand the interplay between curvature and slippage, scaling laws are formulated by analyzing the singularity behaviour of transverse shear flows over perfectly slipping corrugations, a problem important in understanding the limits of superhydrophobic drag reduction. Based on these scaling laws, four different regimes in the interplay are delineated. The resultant effective-slip-length predictions for sinusoidally corrugated surfaces possess comparable simplicity but a wider amplitude-range and intrinsic-slip range of applicability

than those available from literature. A computer-extended regular perturbation theory is also developed, which allows exceptionally accurate predictions even at reasonably large values of the ‘small (amplitude) parameter’.

Confined pressure-driven flows are studied in this thesis using a grid-free semi-analytical approach based on spectral analysis. This method has a faster (exponential) decay of errors compared to discretization-based methods such as finite-differences and finite-elements, and is also easily reducible to new and known analytical forms in various disparate limits. Further, the method brings out crucial physical characteristics of the flow that are inaccessible to asymptotic methods. For example, the permeability in longitudinal flow is shown to transition from faster-than-Poiseuille to slower-than-Poiseuille permeation as pattern pitch is reduced.

The final contribution of this thesis is a spectral-asymptotic approach to model confined flows over complex topographies specifiable by an arbitrary continuous function. Using a novel decomposition of the channel height effects into exponentially and algebraically decaying components, a simple surface-metrology-dependent relationship, which connects the eigenvalues of the effective permeability tensor, is obtained. Representative topographies assessed numerically include the infinitely-differentiable topography of a phase-modulated sinusoid with multiple local extrema and zero-crossings and the non-differentiable triangular-wave topography. Corners in triangular patterns and cusps in scalloped patterns are not found to be an impediment to meaningful and numerically accurate asymptotic predictions, contradicting an earlier suggestion from the literature. Several distinct applications of the theory to the friction-reduction and shear-stability performance of the recently developed lubricant impregnated patterned surfaces and scalloped and trapezoidal drag-reduction riblets are discussed, with comparison to experimental data from the literature for the last application.

## सार

मिश्रण, गीलेपन और घर्षण गुणों के मॉड्यूलेशन और पृथक्करण जैसे उद्देश्यों को प्राप्त करने के लिए स्थलाकृतिक बनावट या सतही गलियारे को अक्सर माइक्रोफ्लुइडिक्स के अनुशासन में नियोजित किया जाता है। माइक्रोफ्लुइडिक्स के बाहर, इस तरह के बनावट अशांत प्रवाह के लिए इंजीनियर खींच के आधारों का निर्माण करते हैं और भूवैज्ञानिक संरचनाओं में तेल या पानी ले जाने वाली खंडित चट्टानों की प्राकृतिक विशेषताएं हैं।

इस तरह के अनुप्रयोगों से प्रेरित, न्यूटन के प्रवाह को स्थलाकृतिक रूप से स्थलाकृतियों के साथ संपर्क स्थापित करने का मैक्रोस्कोपिक लक्षण वर्णन सैद्धांतिक रूप से किया जाता है, जो अपरिवर्तित प्रवाह के लिए एक मीट्रिक के रूप में प्रभावी स्लिप लंबाई टेंसर का उपयोग करता है और सीमित प्रवाह के लिए एक मीट्रिक के रूप में हाइड्रोलिक पारगम्यता पंप। अनुदैर्ध्य के साथ-साथ एक आयामी अंडाकार [धारीदार पैटर्न तक अनुप्रस्थ प्रवाह का विश्लेषण किया जाता है जो वर्णक्रमीय और असममित तरीकों का उपयोग करके किया जाता है। कॉन्टिनम स्केल ने पूरी तरह से हल किए गए परिमित-तत्व सिमुलेशन को असममित भविष्यवाणियों की उपयोगिता का आकलन करने के लिए नियोजित किया है। इस थीसिस में उपयोग किया जाने वाला मुख्य स्पर्शोन्मुख दृष्टिकोण पैटर्न पिच के लिए स्थलाकृतिक पैटर्न की विशेषता आकार के अनुपात को एक छोटे पैरामीटर, आयाम रहित आयाम के रूप में मानता है।

सबसे पहले, कतरनी प्रवाह में sinusoidally नालीदार नो-स्लिप सतहों के लिए, साहित्य से उपलब्ध उन लोगों की तुलना में काफी व्यापक आयाम रेंज पर प्रयोग करने योग्य विश्लेषणात्मक मॉडल विकसित होते हैं, जो सांकेतिक गणनाओं, संख्यात्मक-ग्राफिकल अभिसरण अध्ययनों का लाभ लेते हुए डोम्ब-साइक्स प्लॉट्स और श्रृंखला-यूलर और शैक्स ट्रांसफॉर्मेशन और पेडे सन्निकट जैसी सुधार तकनीकें।

इसके बाद, आंतरिक फिसलन के साथ नालीदार सतहों पर प्रवाह का अध्ययन किया जाता है। वक्रता और फिसलन के बीच परस्पर क्रिया को समझने के लिए, पूरी तरह से फिसलने वाले गलियारों पर अनुप्रस्थ कतरनी प्रवाह की विलक्षणता का विश्लेषण करके स्केलिंग कानून तैयार किए जाते हैं, सुपरहाइड्रोफोबिक ड्रैग रिडक्शन की सीमाओं को समझने में महत्वपूर्ण समस्या। इन स्केलिंग कानूनों के आधार पर, इंटरप्ले में चार अलग-अलग नियम दिए गए हैं। Sinusoidally

नालीदार सतहों के लिए परिणामी प्रभावी-स्लिप-लंबाई भविष्यवाणियों में तुलनीय सरलता है, लेकिन साहित्य से उपलब्ध लोगों की तुलना में व्यापक आयाम-सीमा और प्रयोज्यता की आंतरिक सीमा है। एक कंप्यूटर-विस्तारित नियमित गड़बड़ी सिद्धांत भी विकसित किया गया है, जो 'छोटे (आयाम) पैरामीटर' के यथोचित बड़े मूल्यों पर भी असाधारण सटीक भविष्यवाणियों की अनुमति देता है।

वर्णक्रमीय विश्लेषण के आधार पर ग्रिड-मुक्त अर्ध-विश्लेषणात्मक दृष्टिकोण का उपयोग करके इस थीसिस में सीमित दबाव-संचालित प्रवाह का अध्ययन किया जाता है। इस पद्धति में विवेक-आधारित विधियों जैसे परिमित-अंतर और परिमितताओं की तुलना में त्रुटियों का तेज़ (घातांक) क्षय है, और विभिन्न विषम सीमाओं में नए और ज्ञात विश्लेषणात्मक रूपों के लिए आसानी से पुनर्वितरित किया जाता है। इसके अलावा, विधि प्रवाह की महत्वपूर्ण भौतिक विशेषताओं को सामने लाती है जो कि एसिम्प्टोटिक तरीकों के लिए दुर्गम हैं। उदाहरण के लिए, अनुदैर्घ्य प्रवाह में पारगम्यता को तेज-से-पाँड़जुइल से धीमी-से-पाँड़जुइल पारगमन में बदलने के लिए दिखाया गया है क्योंकि पैटर्न पिच कम हो गया है।

इस थीसिस का अंतिम योगदान एक मनमाना सतत कार्य द्वारा निर्दिष्ट जटिल स्थलाकृतियों पर सीमित प्रवाह के लिए मॉडल के लिए एक वर्णक्रमीय-विषम दृष्टिकोण है। चैनल ऊंचाई के प्रभावों के एक उपन्यास अपघटन का उपयोग घातीय और बीजगणितीय रूप से क्षय करने वाले घटकों में करते हुए, एक सरल सतह-मेट्रोलॉजी-निर्भर संबंध, जो प्रभावी पारगम्यता टेंसर के आइजनवेल्यूज को जोड़ता है, प्राप्त होता है। संख्यात्मक रूप से मूल्यांकन की गई प्रतिनिधि स्थलाकृतियों में कई स्थानीय विलुप्त होने और शून्य-क्रॉसिंग के साथ चरण-संशोधित साइनसॉइड की असीम-अलग-अलग स्थलाकृति और नॉनडिफ़रेन्सेबल त्रिकोणीय-लहर स्थलाकृति शामिल है। त्रिकोणीय पैटर्न में कॉर्न्स और स्कैलपड पैटर्न में क्यूप्स को सार्थक और संख्यात्मक रूप से सटीक विषम भविष्यवाणियों के लिए एक बाधा नहीं पाया जाता है, साहित्य से पहले के एक सुझाव का खंडन। अंतिम अनुप्रयोग के लिए साहित्य के प्रायोगिक डेटा की तुलना के साथ हाल ही में विकसित स्नेहक संसेचित नमूनों वाली सतहों के घर्षण-कटौती और कतरनी-स्थिरता के प्रदर्शन के सिद्धांत के कई अलग-अलग अनुप्रयोगों पर चर्चा की गई है।

# Contents

<b>Abstract</b>	iii
List of Figures	xii
List of Tables	xviii
1 Introduction	1
1.1 The boundary condition to fluid flow on a solid surface . . . . .	2
1.1.1 Navier slip condition on planar surfaces . . . . .	3
1.1.2 Navier’s slip condition on curved surfaces . . . . .	5
1.2 Flow over complex topographies . . . . .	7
1.3 Effective slip . . . . .	9
1.4 Effective permeability . . . . .	11
1.5 Overview of methodologies . . . . .	12
1.5.1 Slight- and slow-variation perturbation theory . . . . .	12
1.5.2 Spectral analysis . . . . .	14
1.5.3 Symbolic computation and series improvement . . . . .	18
1.5.4 Finite-element simulations . . . . .	20
2 Literature Review	22
2.1 Corrugated no slip surfaces . . . . .	23
2.2 Smooth surfaces with intrinsic slip . . . . .	24

2.3	Corrugated surfaces with intrinsic slip with and without curvature effects	25
2.4	Confined flows with constrictions . . . . .	27
2.5	Flow over surfaces with wall patterns of arbitrary shapes . . . . .	27
2.6	Global measures for flow over patterned topographies . . . . .	29
2.6.1	Effective slip length . . . . .	29
2.6.2	Hydraulic permeability and permeability tensor . . . . .	31
2.7	Characterization of flow over topographies using effective slip and effective permeability . . . . .	32
2.8	Modelling approaches . . . . .	35
2.9	Conclusions from the literature review . . . . .	36
2.10	Objectives . . . . .	37
3	Improved Asymptotic Estimates for Effective Slip in Shear Flow over Periodic Topographies	39
3.1	Theoretical model and solution procedure . . . . .	39
3.1.1	Longitudinal flow . . . . .	40
3.1.2	Transverse flow . . . . .	41
3.1.3	Symbolic solution procedure . . . . .	42
3.1.4	Numerical solution procedure . . . . .	43
3.2	Asymptotic prediction versus fully resolved simulation . . . . .	44
3.3	Failure of polynomial approximations . . . . .	45
3.4	Methods for improved asymptotic approximations . . . . .	49
3.4.1	Euler transformation with and without acceleration . . . . .	49
3.4.2	Padé approximants . . . . .	50
3.4.3	Longitudinal flow . . . . .	51
3.4.4	Transverse flow . . . . .	51

3.5	Evaluation of improvement in asymptotic approximation . . . . .	52
3.6	Chapter summary . . . . .	55
4	The Interplay of Curvature-affected Hydrodynamic Slippage with Topographic Patterns in Shear Flow . . . . .	57
4.1	Theoretical model . . . . .	59
4.1.1	Longitudinal Flow . . . . .	60
4.1.2	Transverse flow . . . . .	62
4.2	Polynomial-form asymptotic approximations . . . . .	63
4.3	Shear flow over corrugated surfaces with strong intrinsic slippage . . . . .	65
4.3.1	The zero shear stress surface . . . . .	66
4.3.2	The slip to stick transition and mildly sheared surfaces . . . . .	69
4.3.3	Scaling laws and dominant balances . . . . .	72
4.3.4	Mildly sheared surfaces in transverse flow . . . . .	75
4.4	Higher-order Taylor polynomials versus fully resolved simulation . . . . .	80
4.5	Investigations into convergence limitations of the Taylor polynomials . . . . .	82
4.6	Improvement of polynomial-form asymptotic approximations . . . . .	84
4.6.1	Euler Transformation . . . . .	85
4.6.2	Padé approximants . . . . .	86
4.6.3	Numerical assessment of improved asymptotic approximations . . . . .	87
4.7	Theoretical predictions on the stick-slip transition . . . . .	91
4.8	Chapter summary . . . . .	92
5	Pressure-driven Flows over Sinusoidal Topographies . . . . .	94
5.1	Problem definition . . . . .	94
5.2	Longitudinal Flow . . . . .	95
5.2.1	Spectral Method . . . . .	97

5.2.1.1	Calculation of Discharge . . . . .	99
5.2.2	Useful asymptotic forms . . . . .	100
5.3	Transverse Flow . . . . .	102
5.3.1	Spectral Method . . . . .	104
5.3.1.1	Calculation of Discharge . . . . .	109
5.3.2	Useful asymptotic forms . . . . .	110
5.4	Shear flow limit . . . . .	111
5.5	The lubrication limit . . . . .	114
5.6	Results and discussion . . . . .	114
6	Pressure-driven Flows over Arbitrary-shaped Topographies . . . . .	127
6.1	Theoretical model . . . . .	127
6.1.1	Longitudinal flow . . . . .	130
6.1.1.1	Leading order ( $O(1)$ ): . . . . .	131
6.1.1.2	$O(\epsilon)$ correction: . . . . .	131
6.1.1.3	$O(\epsilon^2)$ correction: . . . . .	132
6.1.1.4	Effective permeability . . . . .	133
6.1.2	Transverse flow . . . . .	136
6.1.2.1	Leading order ( $O(1)$ ) . . . . .	137
6.1.2.2	$O(\epsilon)$ correction: . . . . .	137
6.1.2.3	$O(\epsilon^2)$ correction: . . . . .	138
6.1.2.4	Effective permeability . . . . .	139
6.2	Universal relationship between eigenvalues of the permeability tensor . . . . .	141
6.3	Adaptation of asymptotic findings to other boundary conditions . . . . .	142
6.4	Numerical assessment and applications . . . . .	144
6.4.1	Test Problems . . . . .	146

6.5	Numerical assessment of analytical results . . . . .	149
6.5.1	Extension of the range of accuracy of the asymptotic approximations . . . . .	156
6.5.2	Application to slippery lubricant impregnated surfaces . . . . .	157
6.5.3	Other surface topographies and experimental comparison . . . . .	161
6.6	Chapter summary . . . . .	164
7	Conclusions and Scope for Future Work . . . . .	167
	Bibliography . . . . .	174
A	Supplementary Information for Chapter 3 . . . . .	192
B	Supplementary Information for Chapter 4 . . . . .	194
B.1	The curvature-adjusted Navier slip boundary condition . . . . .	194
B.2	Evaluation of asymptotic predictions from the literature . . . . .	197
B.2.1	Key analytical results from the literature . . . . .	198
B.2.2	Numerical assessment of literature predictions . . . . .	201
B.3	Higher-order Taylor polynomials . . . . .	202
B.4	Euler-transformed polynomials for effective slip length . . . . .	204
B.5	Analytical expressions for effective slip length using Padé approximants . . . . .	205
C	The Slow-variation Approach as an Alternative to the Slight-variation Approach . . . . .	213
C.1	Theoretical Modeling . . . . .	213
C.1.1	Slow Variation Theory (SVT) . . . . .	215
C.2	Slight Variation Theory . . . . .	218
C.2.1	Results and discussion . . . . .	219
D	Supplementary Information for Chapter 5 . . . . .	227

D.1	Asymptotic behaviour of the spectral coefficients . . . . .	227
D.2	Coefficients for the discharge calculated by the fourth-order accurate asymptotic model . . . . .	230
D.2.1	Longitudinal direction . . . . .	230
D.2.2	Transverse direction . . . . .	231
D.3	Additional details on numerical methods . . . . .	232
E	Supplementary Information for Chapter 6	234
E.1	Expressions used for predicting channel height effects in pressure-driven flow with one patterned and one no-slip wall . . . . .	234
E.2	Transverse permeability in free surface and forced-shear confined flows with finite channel-size effects . . . . .	234

# List of Figures

1.1	Examples of microfluidic chips showing microchannels. . . . .	1
1.2	Typo "Perfact" corrected inside figure Interpretation of the Navier slip length $b$ on a flat surface. Source: [1] . . . . .	4
1.3	Graphical representation of Navier slip boundary condition on curved surface.	7
1.4	Different kinds of micro-patterning and application to microscale mixing.	8
1.5	Different kinds of micro-patterning and application to microscale mixing.	9
1.6	Pictorial representation of the effective slip length concept for incompressible creeping flow of a Newtonian fluid across a periodic wall pattern. . .	10
1.7	Definition sketch for slight variation theory (small $\alpha$ ) and slow variation theory (small $\epsilon$ ). . . . .	13
1.8	Decay of Fourier coefficients of discontinuous, non-differentiable and continuous function: An example . . . . .	17
2.1	The local coordinate systems $xoz$ and $x'oz'$ aligned with the stripes and at an angle $\beta$ to the stripes, respectively used to define the effective permeability tensor. . . . .	30
3.1	The geometry and coordinate system for analyzing shear-driven flow over a sinusoidal surface pattern with amplitude $e$ and pitch $L$ , showing the transverse ( $x$ ) and longitudinal ( $z$ ) flow directions. . . . .	40

3.2	Amplitude-dependence of the effective slip length in longitudinal (left pane) and transverse (right pane) flow as evaluated numerically through FRS (Fully Resolved Simulation) . . . . .	45
3.3	Amplitude-dependence of effective slip length as predicted by Taylor polynomials of various degrees compared against numerical simulations using FRS . . . . .	46
3.4	Domb-Sykes plots ( $\frac{A_n}{A_{n-1}}$ vs. $1/n$ ) for flow longitudinal (top pane) and transverse (bottom pane) to the patterns. . . . .	48
3.5	Effective slip predicted by simple Taylor polynomials, polynomials obtained by Euler transformation alone (legend key Euler poly $n$ ), polynomials obtained by Euler transformation accelerated . . . . .	52
3.6	Effective slip length calculated by diagonal Padé approximants of various order evaluated against predictions from fully resolved simulation (FRS). . . . .	53
4.1	The geometry and coordinate system for analyzing shear-driven flow over a sinusoidal surface pattern with amplitude $e$ and pitch $L$ . . . . .	60
4.2	Schematic of the semi-infinite two-dimensional region $S$ over a periodic topography used for the discussion on longitudinal and transverse zero shear flow in Section 4.3.1. . . . .	66
4.3	The effective slip length referred to the mean line as a fraction of intrinsic slip plotted against dimensionless amplitude showing the crossover from slip to stick behaviour. . . . .	70
4.4	Effective slip length referred to the mean line versus dimensionless pattern amplitude ( $\epsilon$ ) for the case of no slip and a relatively large value of slip length ( $B = 7$ ). . . . .	71

4.5	Effective slip predictions from fully-resolved simulations for $B = 3, 5, 7$ shown in symbols compared against predictions from the large- $B$ theory given by Eq. (4.23) shown through solid lines . . . . .	76
4.6	Effective slip predictions from fully-resolved simulations for $B = 3, 5, 7$ shown in symbols compared against predictions from the large- $B$ theory .	77
4.7	Effective slip predictions from fully-resolved simulations for $B = 2, 3, 6$ shown in symbols compared against predictions from the large- $B$ theory .	78
4.8	Effective slip predictions from Taylor polynomials of various degree compared against numerical values using FRS . . . . .	80
4.9	Effective slip predictions from Taylor polynomials of various degree compared against numerical values using FRS in longitudinal (left panes) and transverse (right panes) flow . . . . .	81
4.10	Domb-Sykes plots ( $\frac{A_n}{A_{n-1}}$ vs. $1/n$ ) for flow longitudinal and transverse to the patterns. . . . .	82
4.11	Domb-Sykes plots ( $\frac{A_n}{A_{n-1}}$ vs. $1/n$ ) for flow longitudinal and transverse to the patterns. . . . .	83
4.12	Transverse flow: the variation of the radius of convergence ( $R_c$ ) with respect to intrinsic slip length ( $B$ ) as calculated from Domb-Sykes plots. The black solid line is obtained by curve-fitting a rational approximation. . .	84
4.13	Predictions from three types of approximations having the same formal asymptotic accuracy of $O(\epsilon^n)$ with $n = 4$ , viz. . . . .	87
4.14	Predictions from three types of approximations having the same formal asymptotic accuracy of $O(\epsilon^n)$ with $n = 4$ viz. Taylor polynomials . . . .	88
4.15	Predictions from three types of approximations having the same formal asymptotic accuracy of $O(\epsilon^n)$ with $n = 16$ , viz. Taylor polynomials . . .	89

4.16	Predictions from three types of approximations having the same formal asymptotic accuracy of $O(\epsilon^n)$ . . . . .	90
4.17	Comparison of amplitude-dependence of slip-length calculated by continuum theories against molecular dynamics (MD) simulations [2] for longitudinal (left) and transverse (right) flow. . . . .	91
4.18	The variation of the critical pattern amplitude ( $\epsilon_{crit}$ ) with dimensionless intrinsic slip length ( $B$ ) for longitudinal (left) and transverse (right) flow. . . . .	92
5.1	An infinitely wide channel with sinusoidally patterned lower wall and flat top wall is shown. . . . .	95
5.2	Longitudinal flow: Variation of the scaled permeability of the channel with dimensionless pattern amplitude ( $\alpha$ ) for different dimensionless wavelengths ( $\lambda$ ). . . . .	115
5.3	Transverse flow: Variation of the scaled permeability of the channel with dimensionless pattern amplitude ( $\alpha$ ) for different dimensionless wavelengths ( $\lambda$ ). . . . .	117
5.4	Variation of dimensionless hydraulic permeability with a scaled minimum spacing between patterned and unpatterned plates for two patterns with different amplitude to pitch ratios . . . . .	120
5.5	Variation of permeability with dimensionless pattern wavelength, showing comparison between spectral model predictions . . . . .	122
5.6	The variation of effective slip length with the amplitude to wavelength ratio ( $\epsilon$ ) in longitudinal (left pane) and transverse (right pane) flow . . . . .	123
5.7	The variation of effective slip length with the amplitude to wavelength ratio ( $\epsilon$ ) . . . . .	125

6.1	The longitudinal/transverse flows through a channel with an arbitrarily shaped pattern on the bottom wall and a flat top wall. . . . .	128
6.2	Surface topography shapes for the two test cases . . . . .	147
6.3	Variation of effective permeability with dimensionless characteristic pattern size ( $\epsilon$ ) in longitudinal (left panel) and transverse flow (right panel)	151
6.4	Variation of effective permeability with dimensionless characteristic pattern size ( $\epsilon$ ) in longitudinal (left panel) and transverse flow (right panel) for $a = \pi/2$ and $H = \pi/4$ in Topography A. . . . .	153
6.5	Variation of effective permeability with dimensionless characteristic pattern size ( $\epsilon$ ) in longitudinal (left panel) and transverse flow (right panel) for different values of $H$ in Topography B. . . . .	154
6.6	Demonstration of range extension through use of (1,2) Padè approximant (dashed lines) and polynomial form (solid lines) for triangular grooves with $H = 2\pi$ . . . . .	157
6.7	The top left panel shows a schematic of a pitch-averaged gas/lubricant cushion model of effective slip for hydrodynamic characteristics . . . . .	158
6.8	Trapezoidal and scalloped topographies . . . . .	163
B.1	Comparison of amplitude-dependence of effective slip predicted by models available from the literature with predictions from fully-resolved simulations using FEM (red symbols) for the dimensionless slip length values $B = 0.1$ (top row) and $B = 0.5$ (bottom row). . . . .	200
B.2	Comparison of amplitude-dependence of effective slip predicted by models available from the literature with predictions from fully-resolved simulations using FEM (red symbols) for the dimensionless slip length values $B = 1$ (top row) and $B = 3$ (bottom row). . . . .	201

C.1	Flow through a channel with sinusoidally patterned top wall and flat bottom wall. . . . .	214
C.2	Variation of non-discharge ratio with dimensionless amplitude ( $\alpha$ ) for six different dimensionless wavelength ( $\lambda$ ). . . . .	220
C.3	Symbols indicate numerical predictions (FRS). Solid curve indicates predictions from extended slow variation theory (ESVT) using Eq. (C.18). . . . .	223
C.4	Depth-wise variation of velocity for $\lambda = 4$ at one transverse ( $Z$ ) location for $\alpha = 0.5$ , calculated using SVT, ESVT and numerical simulation (FRS). . . . .	224
C.5	Velocity variation with transverse coordinate ( $Z$ ) on a surface at a constant normal distance $0.1h_0$ from the wall as predicted numerically (FRS) and by SVT, ESVT and SAT. . . . .	225

# List of Tables

1.1	Fourier coefficients of various functions and their asymptotic forms for large $n$ . Appearance of functions $\exp$ and $\cos$ made consistent with rest of the thesis . . . . .	15
1.2	Comparison between two specific values of $\log(1 + \epsilon)$ predicted by the corresponding truncated eight term power series $\sum_{n=1}^8 \epsilon^n/n$ denoted as ‘Taylor poly 8’ . . . . .	20
4.1	Understanding curvature effects in transverse flow through the asymptotic behaviour of the dimensionless intrinsic slip length and the consequent relative significance of the terms . . . . .	74
4.2	Effective slip length calculated on the basis of different scaling laws between $B$ and $\epsilon$ , Here, $B_i$ with $i = 1, 2, 3, 4$ are $O(1)$ quantities defined by the scaling formulas in the first column. . . . .	75
6.1	The Fourier coefficients and sums required for large- $H$ permeability evaluation with trapezoidal and scalloped topographies shown in Fig. 6.8. The parameter $a < \pi/2$ for the trapezoidal profile. . . . .	164
B.1	Padé(8,8) for various slip length $B$ in longitudinal ( $Ln$ ) and transverse ( $Tr$ ) flow. . . . .	207
C.1	variation of dimensionless hydraulic permeability and velocity at the point ( $y = 0.95, z = 0$ ) for $\lambda = 1$ and $\alpha = 0.9$ with respect to different mesh sizes.	219